

Monophosphanes and Diphosphanes with the Hypersilyl Substituent

Vittorio Cappello,^[a] Judith Baumgartner,^{[a][‡]} and Alk Dransfeld,^{[a][‡]} and Karl Hassler^{*[a]}

Keywords: Hypersilylphosphanes / Potassium phosphanides / Ab initio calculations / *P*-Silylhalophosphanes / Silicon

The synthesis of $(\text{SiMe}_3)_3\text{SiPH}_2$ (**1**) (further on denoted as hypersilylphosphane, HypPH_2) was achieved by two methods: by the reaction of $(\text{SiMe}_3)_3\text{Si}(\text{OSO}_2\text{CF}_3)$ with PH_3 , and alternatively, by the reaction of NaPH_2 with $(\text{SiMe}_3)_3\text{SiCl}$ (hypersilylchloride). The latter reaction also afforded bis(hypersilyl)phosphane Hyp_2PH (**2**). By the reaction of **1** and known hypersilylbis(trimethylsilyl)phosphane (**3**) with *t*BuOK, the novel hypersilylphosphanides HypPHK (**4**) and $\text{Hyp}(\text{SiMe}_3)\text{-PK}$ (**5**) were prepared. Compound **1** also reacted with *n*BuLi to form HypPHLi (**6**) and HypPLi_2 (**7**). Furthermore, **3** reacted with hexachloroethane and 1,2-dibromotetrachloroethane to give $\text{HypPCl}(\text{SiMe}_3)$ (**8**) and $\text{HypPBr}(\text{SiMe}_3)$ (**9**) as well as HypPCl_2 (**10**) and HypPBr_2 (**11**). Compounds **4** and **5** reacted smoothly with 1,2-dibromoethane to give diphosphane HypHPPHHyp (**12**) as a mixture of the *meso*- and *rac*-D,L-diastereomers and $\text{Hyp}(\text{SiMe}_3)\text{PP}(\text{SiMe}_3)\text{Hyp}$ (**13**) as the D,L-modification only. By reducing the known compound *t*BuHypPCl with potassium, the D,L-modification of

*t*BuHypPPHyp*t*Bu (**14**) was obtained. All compounds were characterized by ^{29}Si - and ^{31}P NMR spectroscopy and elemental analyses with the exception of the phosphanides which were characterized spectroscopically only. The crystal structures of **3** and **4** and of diphosphanes **10**, **11** and **13** are reported. From temperature-dependent ^{31}P NMR experiments, the coalescence temperature for the *meso*↔D,L interconversion of **12** was determined at 110 °C and gave an inversion barrier of roughly 69.4 kJ mol⁻¹, which is corroborated by results of ab initio calculations at the B3LYP/6-31G(d) level. Two diastereomeric inversion transition structures for diphosphanes R-PH-PH-R with either a *syn* or an *anti* arrangement of the P-H bond and the phosphorus lone pair of electrons could be located; bulky substituents seem to prefer the *anti* arrangement.

(© Wiley-VCH Verlag GmbH & Co. KGaA, 69451 Weinheim, Germany, 2006)

Introduction

The bulky tris(trimethylsilyl)silyl group, often denoted as the hypersilyl group [a term coined by Nils Wiberg^[1] to distinguish it from the tri(*tert*-butyl)silyl group which he named supersilyl], has been used extensively in the past to stabilize and protect uncommon bonding states of main group elements and transition elements. Despite the bulkiness of the group, a number of geminal dihypersilyl derivatives were also synthesized successfully, essentially with heavier main group elements. We will not give a full account of all the compounds that have been prepared so far, as this can be found in refs.^[2–4] and the literature cited therein. K. Klinkhammer even succeeded to synthesize NaSnHyp_3 , the only known compound with three hypersilyl groups on one central atom.^[5]

Despite this widespread use of the hypersilyl group, the number of known hypersilyl compounds of the elements of

group V (N, P, As, Sb, and Bi) is surprisingly small. With nitrogen, HypNH_2 , HypNHLi , $\text{HypNH}(\text{SiMe}_3)$ and $\text{HypNLi}(\text{SiMe}_3)$ have been described,^[6] and some derivatives such as tris(trimethylsilyl)silylamides of zinc,^[7] tin and mercury have also been reported.^[8]

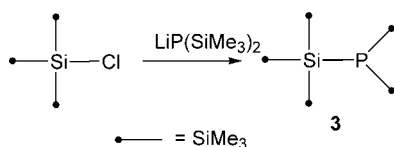
The first hypersilyl phosphorus compound, HypPtBuCl , was described by Cowley.^[9] It is a thermally stable silylhalophosphane that undergoes a silicon-halogen exchange reaction at about 100 °C. Hypersilyldiphenylphosphane was prepared for mass spectroscopic purposes in 1993.^[10] Regitz et al. introduced the hypersilyl group into 1*H*-phosphirenes, which undergo isomerization to furnish trimethylsilyl-substituted phosphasiletanes upon irradiation.^[11] Klingebiel reported the preparation of stable hypersilylfluorophosphanes that have an amino group as the third substituent on the P atom, for instance $(\text{SiMe}_3)_2\text{N}$.^[12] The synthesis of $\text{HypPMe}(\text{NRP}=\text{NR})$ with $\text{R} = 2,4,6-(\text{Me}_3\text{C})_3\text{C}_6\text{H}_2$ was reported in 1991.^[13] Recently, C. Marschner reported the synthesis of a bis(hypersilyl)phosphane, Hyp_2PNR .^[14]

In our group, bis(trimethylsilyl)hypersilylphosphane was prepared some years ago by the reaction of bis(trimethylsilyl)lithiumphosphanide with hypersilylchloride (Scheme 1).^[15]

[a] Institute of Inorganic Chemistry, University of Technology, Stremayrgasse 16, 8010 Graz, Austria
E-mail: vittorio.cappello@tugraz.at
judith.baumgartner@tugraz.at
alk.dransfeld@tugraz.at
karl.hassler@tugraz.at

[‡] X-ray structures

[‡‡] Ab initio calculations



Scheme 1.

Recently, we also reported the synthesis of air-stable tri(hypersilyl)heptaphosphane,^[16] which undergoes an interesting reaction with *t*BuOK even at temperatures as low as $-60\text{ }^{\circ}\text{C}$. In the first step of the reaction, a silicon–silicon bond is cleaved with concomitant formation of *t*BuOSiMe₃. The resulting potassium silanide rearranges into a heptaphosphanide anion and bis(trimethylsilyl)silylene that inserts into a P–P bond of the three-membered ring at the base of the P₇-cage.^[17]

At present, no compounds with the hypersilyl group attached to arsenic, antimony or bismuth are known.

The desire to have at our disposal some hypersilyl–phosphorus synthons which can be used widely, for instance for the preparation of hypersilyldiphosphanes and hypersilyl oligophosphanes, motivated us to investigate various possibilities for the preparation of HypP(SiMe₃)X and HypPX₂, (X = halogen), HypPHK and HypP(SiMe₃)K. Here we report on the successful synthesis of these phosphanes and phosphanides as well as on some reactions they can undergo.

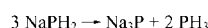
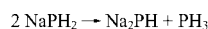
Results and Discussion

Syntheses

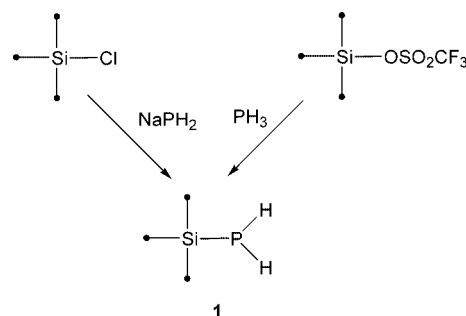
Synthesis of HypPH₂ (1) and (Hyp)₂PH (2)

Reactions of silyltriflates with PH₃ that form Si–P bonds were first described by W. Uhlig.^[18] We transferred this methodology to the synthesis of (SiMe₃)₃Si(OSO₂CF₃) (prepared from (SiMe₃)₃SiPh^[19] and HOSO₂CF₃), which reacts cleanly with PH₃ in the presence of triethylamine to give HypPH₂ in almost quantitative yield. No disubstitution with the hypersilyl group at the phosphorus atom could be observed in this reaction. An alternative route starts from NaPH₂, which can be prepared from PH₃ and sodium in liquefied ammonia.^[20] If the reaction is heated at reflux in toluene, (SiMe₃)₃SiCl and NaPH₂ slowly react over a period of a week to give a 1:1 mixture of hypersilyl- and dihypersilylphosphane (Scheme 2).

As minor byproducts of the reaction that are easily identified with ³¹P NMR spectroscopy, HypPHHPHyp and P₇Hyp₃ are also formed, probably through the decomposition of NaPH₂ at $110\text{ }^{\circ}\text{C}$:



As HypPH₂ and (Hyp)₂PH can easily be separated and purified by fractional sublimation in vacuo, this procedure simultaneously affords both phosphanes on a preparative scale.



Scheme 2.

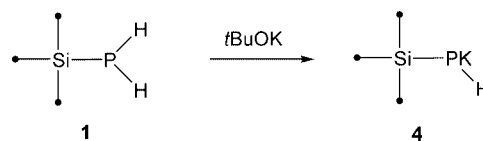
Synthesis of HypPHK (4), HypP(SiMe₃)K (5), and HypPHLi (6)

It is well known from the work of G. Fritzl^[21] that P–Si bonds can be cleaved by alkyl lithium reagents to form silylated Li-phosphanides. However, these phosphanides are not very stable at room temperature. For instance, (SiMe₃)₂PP(SiMe₃)Li decomposes quickly to form a plethora of compounds such as P(SiMe₃)₃, LiP(SiMe₃)₂ and Li₃P.

To obtain some understanding of the thermal stability of hypersilyllithiumphosphanides, we treated HypPH₂ with *n*BuLi in THF at $-60\text{ }^{\circ}\text{C}$. As expected, the only initial product that was formed was HypPHLi, which decomposed slowly to form HypP(SiMe₃)Li and HypPLi₂ as well as (SiMe₃)₂PLi besides some other unidentified products. The intensity of the signal in the ³¹P NMR spectrum of HypPHLi gradually diminished with time.

We therefore chose to investigate the reaction of HypPH₂ with *t*BuOK. Though *t*BuOK is known to cleave P–Si bonds of P(SiMe₃)₃^[22] to give (SiMe₃)₂PK and *t*BuOSiMe₃, it was our expectation that the hypersilyl group might not be attacked due to its bulkiness and that PH would be transformed into PK.

As could easily be followed by ³¹P NMR spectroscopy, the reaction cleanly gave HypPHK in about 90% yield in THF. A minor byproduct of the reaction was HypPK₂, besides some HypPH₂ (Scheme 3). Most importantly, HypPHK turned out to be stable for more than a week at room temperature. It can be crystallized from hexane in the presence of 18-crown-6 for further purification.

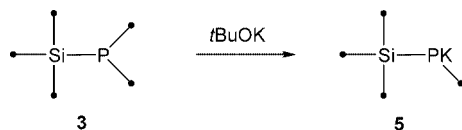


Scheme 3.

Because of the bulkiness of the hypersilyl group, *t*BuOK reacts with HypP(SiMe₃)₂ by the cleavage of only one trimethylsilyl group to form HypPK(SiMe₃) in excellent yields (>90%). As a minor byproduct, HypPHK was always present in the reaction mixtures. HypPK₂ can also be obtained from HypP(SiMe₃)₂ by adjusting the stoichiometry, albeit in moderate yields.

Synthesis of HypP(SiMe₃)H

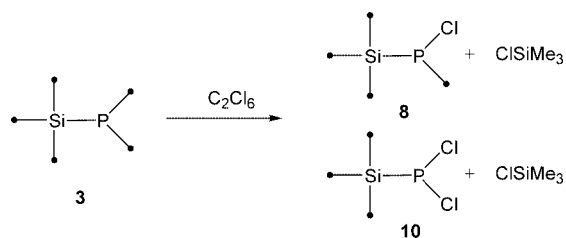
Over a period of three weeks, **3** (Scheme 4) reacts slowly with *t*BuOH at room temperature to form HypP(SiMe₃)H and Me₃SiO*t*Bu as a byproduct. No cleavage of the hypersilyl–phosphorus bond occurs, and no HypPH₂ can be detected in the reaction mixture. HypP(SiMe₃)H is easily separated from unreacted **3** by vacuum sublimation.



Scheme 4.

Synthesis of HypPX(SiMe₃) and HypPX₂, X = Cl, Br (**8**, **9**, **10**, **11**)

By the reaction of *t*BuP(SiMe₃)₂ with C₂Cl₆, Appel^[23] et al. were able to prepare *t*BuP(SiMe₃)Cl, the first moderately stable P-chloro–P-silylphosphane with *t*_{1/2} ≈ 13 min at ambient temperature. We were curious to know if the substitution of the *t*Bu group with hypersilyl would also give stable chlorosilylphosphanes, which it did. The synthesis was achieved by the reaction of HypP(SiMe₃)₂ with one or two equiv. of C₂Cl₆ (Scheme 5). All attempts to crystallize the samples failed despite the fact that the compounds were formed in excellent yields.

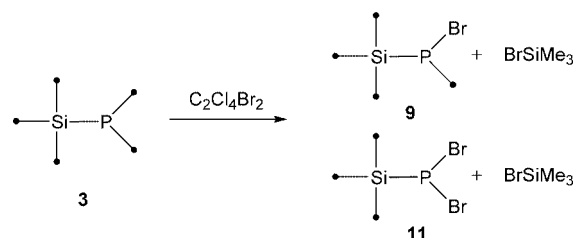


Scheme 5.

The chlorodisilylphosphane turned out to be astonishingly stable and survived several days heated at 70 °C as a solution in toluene. When heated at reflux in toluene, it decomposed quickly to give a plethora of unidentified products. From the observed shifts in the ³¹P NMR spectra it can be concluded that some of these products contain P–P bonds, which supports the evidence that ClSiMe₃ is eliminated with concomitant formation of hypersilylphosphanylidene which then undergoes all sorts of insertion reactions. It is of some note that no change in colour occurred upon the thermal elimination of ClSiMe₃. The thermal stability of the compound is noticeably decreased in THF, where decomposition occurs at a temperature as low as 40 °C.

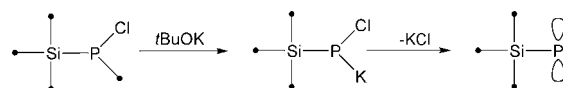
HypP(SiMe₃)₂ reacts cleanly and quantitatively with BrCl₂CCl₂Br to form HypPBr(SiMe₃) (**9**) and HypPBr₂ (**11**), which are both fairly stable at room temperature (Scheme 6). We were unable to obtain crystals of these two silylhalophosphanes that were suitable for X-ray diffraction experiments. When HypP(SiMe₃)Cl reacts with BrCl₂CCl₂Br, a mixture of HypPBr₂ and HypPClBr

(≈ 90:10) forms, which can be observed by analysis of the ³¹P NMR spectrum.



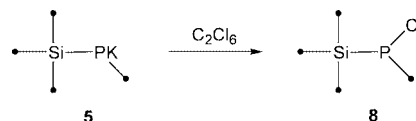
Scheme 6.

As reported elsewhere, HypP(SiMe₃)Cl is an excellent precursor to hypersilylphosphanylidene.^[24] When it is added dropwise to a solution of *t*BuOK in THF, the colour changes immediately to brown and then to a deep violet and the triphosphaallyl anion [Hyp₂P₃][−] forms. By reversing the procedure, bis(hypersilyl)diphosphane is formed when a solution of *t*BuOK is added to a solution of HypP(SiMe₃)Cl by dimerization of hypersilylphosphanylidene which is generated under these reaction conditions (Scheme 7).



Scheme 7.

The reaction of HypP(SiMe₃)K (**5**) with C₂Cl₆ does not give HypPClK through Si–P bond cleavage, followed by KCl elimination and formation of the phosphanylidene HypP. Instead, chlorophosphane **8** is formed quantitatively (Scheme 8). A diphosphane is also not formed by the reaction of unreacted **5** with **8**.



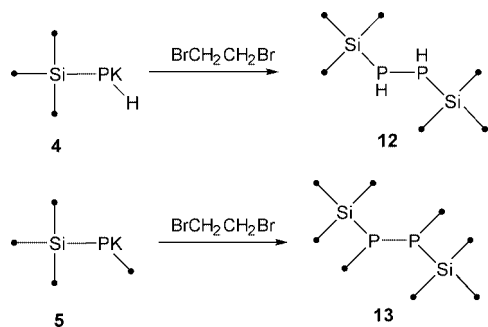
Scheme 8.

Attempts to prepare a disilylfluorophosphane, HypP(SiMe₃)F, by the reaction of **5** with FCl₂CCl₂F were unsuccessful.

Synthesis of (Hypersilyl)diphosphanes

HypPHK and HypPK(SiMe₃) cleanly react with 1,2-dibromoethane to give the bulky diphosphanes HypPHHPHy (**12**) and Hyp(SiMe₃)PP(SiMe₃)Hy (**13**) (Scheme 9). As follows from the ³¹P NMR spectra, 1,2-dihypersilyldiphosphane forms as a mixture of *meso*- and *rac*-D,L-diastereomers which differ in their ³¹P–³¹P coupling constants (see section NMR spectroscopy). 1,2-Bis(hypersilyl)-1,2-bis(trimethylsilyl)diphosphane shows a single resonance in the ³¹P NMR spectrum that originates from the D,L-diastereomers. This interpretation is corroborated by the X-ray structure.

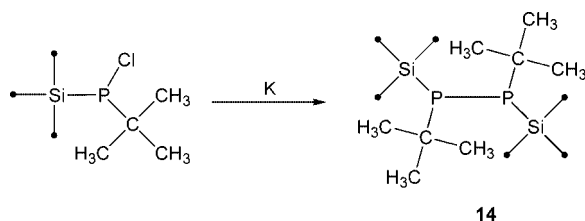
We also investigated the reaction of HypPH₂ with *t*Bu₂Hg in an attempt to prepare a cyclotetraphosphane



Scheme 9.

which is known to form when $(\text{SiMe}_3)\text{PH}_2$ is used.^[25] Because of the bulkiness of the hypersilyl group, the reaction stops with the formation of bis(hypersilyl)diphosphane even when an excess of $t\text{Bu}_2\text{Hg}$ is used. Here again, a mixture of the *meso*- and *rac*-D,L-diastereomers is formed.

By reducing the known compound $t\text{Bu}(\text{Hyp})\text{PCl}$ ^[9] with potassium, we were able to prepare the even bulkier diphosphane $t\text{Bu}(\text{Hyp})\text{PP}(\text{Hyp})t\text{Bu}$ (**14**), which again possesses a single resonance in the ^{31}P NMR spectrum (Scheme 10). X-ray diffraction experiments again show that it is the D,L-racemic modification that is formed.



Scheme 10.

We will report on our attempts to prepare tetra(hypersilyl)diphosphane in a forthcoming paper.

^{29}Si and ^{31}P NMR Spectroscopy

Shift Data and Coupling Constants

All compounds were characterized by ^{29}Si - and ^{31}P NMR spectroscopy. The relevant shift data and the coupling constants are summarized in Table 1, which includes data for compounds that were not isolated in their pure form such as HypPClBr .

^{31}P NMR Spectrum and Inversion Barrier of Bis(hypersilyl)diphosphane (**12**)

Figure 1 presents the experimental proton-coupled ^{31}P - and ^1H NMR spectra of **12** which both display two AA' (or XX') subspectra of two AA'XX' spin systems ($\text{A} = \text{P}$, $\text{X} = \text{H}$) originating from the *meso*- and *rac*-D,L-**12** and the racemic modification. The coupling with the hypersilyl protons is negligibly small, which causes a broadening of the lines only. Because of the size of the hypersilyl group, all diastereomers are expected to adopt the *anti* conformation only at room temperature to minimize the steric repulsion between the two hypersilyl groups (see section X-ray Crystallography).

As Figure 2 shows, with the help of Newman projections, the two phosphorus lone pairs of electrons will be *trans* ($\omega \approx 180^\circ$) to each other for the *meso* form and *gauche* ($\omega \approx 60^\circ$) to each other for the D,L-diastereomer. As is known from numerous studies, the absolute value of the one bond P–P coupling constant $|^1J_{\text{P,P}}|$ is large for a *gauche* arrangement of the lone pairs of electrons and comparatively small for the *trans* arrangement.^[26] For instance, ab initio calculations at the B3LYP/6-31+G**/B3LYP/IGLO-III level of theory for 180° and 60° electron lone pair dihedral angles of P_2H_4 predict $^1J_{\text{P,P}}$ values of +2.5 and -187.9 Hz, respectively.^[27] For *meso*-1,2-di(*tert*-butyl)diphosphane, -162.7 Hz is reported in the literature and -206.6 Hz is reported for the D,L-diastereomer.^[28]

Table 1. Chemical shifts $\{[\text{ppm}], \delta(^{29}\text{Si}) \text{ against TMS}, \delta(^{31}\text{P}) \text{ against } \text{H}_3\text{PO}_4\}$, and coupling constants [Hz] for hypersilylmonophosphanes and hypersilyldiphosphanes.

Compound	No.	Solvent	Hypersilyl group						SiMe ₃ group				
			$\delta(^{31}\text{P})$	$\delta(^{29}\text{Si}^*)$	$\delta(^{29}\text{Si})$	$^1J(\text{PSi}^*)$	$^2J(\text{PSi})$	$^2J(\text{Si}^*\text{H})$	$\delta(^{29}\text{Si})$	$^1J(\text{PSi})$	$^1J(\text{P,H})$	$^2J(\text{P,H})$	$^1J(\text{P,P})$
HypP(SiMe ₃) ₂	3	toluene	−268.8	−100.2	−10.5	90.5	8.8	—	+3.6	32.4	—	—	—
HypPH(SiMe ₃)		toluene	−257.3	−101.5	−10.6	65.5	10.1	—	+3.9	32.2	—	—	—
HypPH ₂	1	toluene	−265.4	−102.4	−11.8	46.7	9.0	0.6	—	—	178.7	—	—
Hyp ₂ PH	2	toluene	−272.0	−93.9	−10.0	88.7	11.4	16.4	—	—	195.1	—	—
HypPHK	4	THF	−352.9	−91.4	−14.5	98.5	11.9	1.1	—	—	144.3	—	—
HypPHLi	6	THF	−358.2	−94.6	−14.1	85.9	10.6	1.1	—	—	144.3	—	—
HypPK(SiMe ₃)	5	toluene	−352.7	−94.6	−14.1	121.9	11.2	—	+0.7	9.1	—	—	—
HypPK ₂		toluene	−367.4	−76.7	−17.1	107.9	13.9	—	—	—	—	—	—
HypPLi ₂	7	THF	−371.4	—	—	—	—	—	—	—	—	—	—
<i>meso</i> -[HypPH] ₂	12	toluene	−202.0	−93.7	−9.6	29.0 ^[a]	8.0 ^[a]	—	—	—	170.6	15.9	−80.9
D,L-[HypPH] ₂	12	toluene	−212.0	−94.4	−9.5	26.5 ^[a]	7.0 ^[a]	—	—	—	171.9	12.0	−254.1
D,L-[HypP(SiMe ₃)] ₂	13	toluene	−201.2	−82.3	−9.4	35.9 ^[a]	10.5 ^[a]	—	+4.5	28.7	—	—	—
D,L-[HypP(<i>t</i> Bu)] ₂	14	toluene	−41.8	−83.0	−9.8	46.0 ^[a]	12.3 ^[a]	—	—	—	—	—	—
HypP(SiMe ₃)Cl	8	toluene	+38.1	−83.5	−8.6	102.3	12.2	—	+9.3	51.3	—	—	—
HypP(SiMe ₃)Br	9	toluene	+7.5	−84.3	−8.5	103.2	12.0	—	+7.3	54.4	—	—	—
HypPCl ₂	10	toluene	+236.2	−62.8	−8.8	103.8	14.6	—	—	—	—	—	—
HypPBr ₂	11	toluene	+206.5	−62.0	−7.1	108.6	15.3	—	—	—	—	—	—
HypPBrCl		toluene	+222.9	—	—	—	—	—	—	—	—	—	—

[a] Pseudotriplet, given is the observed line spacing.

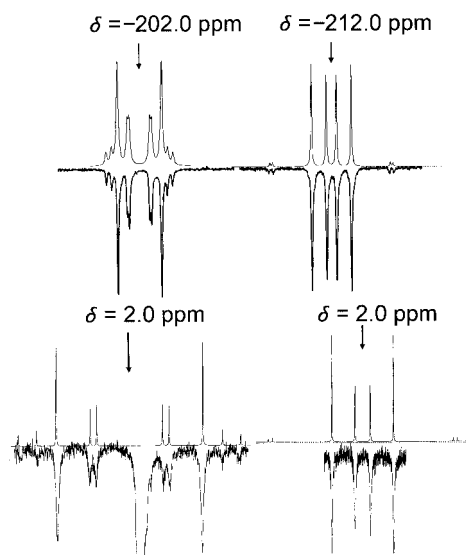


Figure 1. Calculated (positive intensities) and observed ^{31}P - (top) and ^1H NMR spectra of *meso*- (-202.0, 2.0 ppm, respectively) and *D,L*-bis(hypersilyl)diphosphane (-212.0, 2.9 ppm).

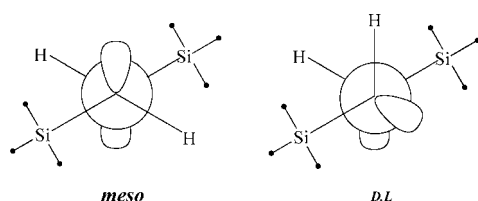


Figure 2. Newman projections for the *anti* conformers [$\omega(\text{Si-P-P-Si}) \approx 180^\circ$] of *meso*- and *D,L*-HypPHHPHyp.

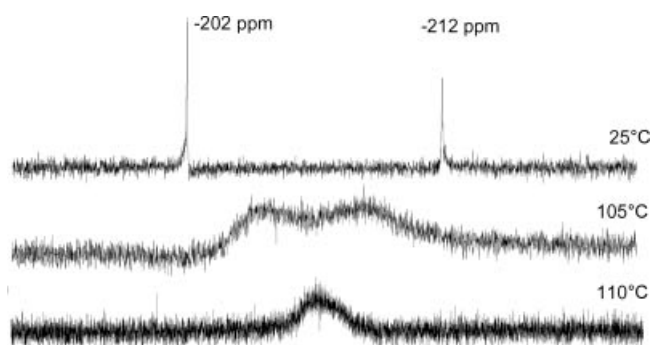


Figure 3. Proton-decoupled ^{31}P NMR spectrum of a solution of **12** in toluene at three different temperatures. The frequency separation $\delta\nu$ at 25°C is 1214.2 Hz.

From the simulated spectra, $^1J_{\text{P,P}}$ values of -80.9 Hz are obtained for the *meso*-diastereomer, and -254.1 Hz for the *D,L*-diastereomer. The difference is much larger than that of 1,2-di(*tert*-butyl)diphosphane, but it is close to the difference calculated for P_2H_4 .

Figure 3 presents the proton-decoupled ^{31}P NMR spectrum of a solution of **12** in toluene at three different temperatures. Coalescence due to rapid interconversion of

meso \leftrightarrow *D,L* occurs at $T_c = 110^\circ\text{C}$. ΔG^\ddagger can be approximated by $\Delta G^\ddagger = 19.13 T_c(9.97 + \log T_c/\delta\nu)^{[29]}$, the barrier for phosphorus inversion can be estimated to be 69.4 kJ mol $^{-1}$.

Ab initio Calculation of the Phosphorus Inversion Barrier of **12**

Dynamic NMR experiments have been used for the determination of the inversion barriers (ΔE_{inv}) of silylphosphanes as early as 1970. For $\text{C}_6\text{H}_5\text{P}(\text{iPr})\text{SiMe}_3$ and $\text{C}_6\text{H}_5\text{P}(\text{SiMe}_2\text{H})_2$ values of 78 and 51 kJ mol $^{-1}$ were reported, respectively. $^{[30,31]}$ These are smaller than those obtained for organophosphanes. The observed lowering of ΔE_{inv} upon silyl substitution has been related to three effects, which include a destabilization of the pyramidal structure and a stabilization of the transition structure by either π -acceptor or σ -donor properties. $^{[32]}$ Earlier ab initio calculations by one of the authors (A. Dransfeld $^{[33]}$) predicted that replacement of a hydrogen atom of PH_3 with PH_2 ($\text{PH}_3 \rightarrow \text{H}_2\text{PPH}_2$) is accompanied by a lowering of ΔE_{inv} from 147.9 to 114.1 kJ mol $^{-1}$. Thus, disilyldiphosphanes, RHPHR, are predicted to possess even smaller barriers than those of organophosphanes, which is fully confirmed by the NMR results of **12**.

To gain some deeper understanding of the nature of the inversion barrier of disilyldiphosphanes, ab initio calculations for a small series of representative species, RHPHR with $\text{R} = \text{H}, \text{Me}, \text{CMe}_3, \text{SiH}_3, \text{Si}(\text{SiH}_3)_3$ and $\text{Si}(\text{SiMe}_3)_3$, have been performed at the B3LYP/6-31G* level of theory. Optimized transition structures were evaluated on the basis of the analysis of vibration modes at the same level of theory.

An interesting feature of the inversion of these diphosphanes is the occurrence of two alternative, diastereomeric transition structures which we term *anti* and *syn* as they differ by the dihedral angle between the lone pair of electrons at the pyramidal P atom and the P–H bond of the planar (inverting) P atom. Schematic drawings of these structures are presented in Figure 4, and relative energies as well as Mulliken charges of the phosphorus atoms are summarized in Table 2. The reader may note that the *anti* TS of diphosphane $\text{P}_i\text{RH-P}_p\text{RH}$ with the (*R*) configuration at P_p is enantiomeric to the *anti* TS of the corresponding diphosphane with the (*S*) configuration at P_p . Therefore, the energy of the *anti* TS and the *syn* TS in Table 2 are independent of the chirality at P_p .

For small substituents $\text{R} = \text{Me}$ and SiH_3 , the *syn* transition structure is preferred, as seen from Table 2. With increasing bulkiness of the substituent [$\text{R} = \text{CMe}_3, \text{Si}(\text{SiH}_3)_3$ and $\text{Si}(\text{SiMe}_3)_3$], the *anti* transition structure with an approximate 180° dihedral angle between the lone pair of electrons at the pyramidal phosphorus and the P–H bond at the inverting P atom becomes lower in energy. Although the preference for the *anti* structure for large R groups is sufficiently explained by steric arguments, the preference for the *syn* geometry in the case of $\text{R} = \text{methyl}$ is due to conjugation of the lone pair of electrons at the pyramidal P atom with the antibonding $\sigma(\text{P}_i\text{H})$ orbital.

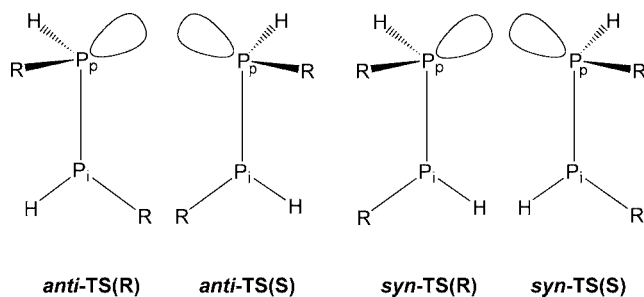


Figure 4. Schematic representation of the *anti* and *syn* transition structures of diphosphanes RHP-PHR. P_i denotes the planar P atom that undergoes inversion, P_p the pyramidal phosphorus atom.

Table 2. Relative energies [kJ mol^{-1}] and Mulliken charges Q of the P atoms for the *anti* and *syn* transition states of diphosphanes RHP-PHR and of monophosphanes $\text{H}_2\text{P-R}$. P_i denotes the inverting P atom.

R	RHP-PHR				$\text{H}_2\text{P-R}$		
	E_{rel}	Type of TS	$Q(P_i)$	$Q(P_p)$	E_{rel}	Type of TS	$Q(P)$
H	116.4	<i>anti</i> = <i>syn</i>	0.03	-0.25	148.8		-0.27
CH_3	113.3	<i>anti</i>	0.16	-0.11	149.7	<i>eclipsed</i>	-0.14
CH_3	112.1	<i>syn</i>	0.16	-0.12			
CMe_3	99.3	<i>anti</i>	0.14	-0.12	147.6	<i>eclipsed</i>	-0.16
CMe_3	100.9	<i>syn</i>	0.15	-0.13			
SiH_3	80.1	<i>anti</i>	-0.07	-0.32	104.8	<i>eclipsed</i>	-0.33
SiH_3	79.4	<i>syn</i>	-0.06	-0.33			
SiMe_3	72.2	<i>anti</i>	-0.12	-0.35	96.6	<i>eclipsed</i>	-0.38
SiMe_3	75.5	<i>syn</i>	-0.10	-0.37			
$\text{Si}(\text{SiH}_3)_3$	76.9	<i>anti</i>	-0.02	-0.27	103.6	<i>gauche</i>	-0.29
$\text{Si}(\text{SiH}_3)_3$	80.6	<i>syn</i>	-0.02	-0.28			
$\text{Si}(\text{SiMe}_3)_3$	74.8	<i>anti</i>	-0.08	-0.33	98.9	<i>gauche</i>	-0.36
$\text{Si}(\text{SiMe}_3)_3$	97.2	<i>syn</i>	-0.08				

With a value of 74.8 kJ mol^{-1} , the calculated inversion barrier of **12** is in excellent agreement with the experimental value and also fits nicely into trends observed for various R substituents. As reported previously,^[33] methyl substituents reduce the inversion barrier more than PH_3 does, which is due to electronic effects (σ -acceptor), and *t*Bu decreases the barrier because it destabilizes the steric effects in the pyramidal minimum structure. A distinct lowering of ΔE_{inv} occurs for a silyl group because of its σ -donor character. Additional steric effects in the minimum structure further reduce ΔE_{inv} in $\text{H}_2\text{P-SiMe}_3$. Noteworthy, further increase of the bulkiness of R in H_2PR does not lower the barrier more than $\text{H}_2\text{P-SiMe}_3$. In general, donation from the substituent is reflected in the phosphorus charge in the transition state of all of the $\text{H}_2\text{P-SiX}_3$ molecules. The more negatively charged the P atom is in the TS, the lower the ΔE_{inv} . To quantify these trends, results of the calculations for the monophosphanes H_2PR ($\text{R} = \text{CX}_3$ or SiX_3) have been included in Table 2. Here again, transition structures for different R groups are observed which differ in the dihedral angle ω between a P-H and a C-X or Si-X bond, which

we term *syn* ($\omega \approx 0^\circ$) and *gauche* ($\omega \approx 60^\circ$) as shown in Figure 5. For large R groups, the *gauche* TS is adopted.

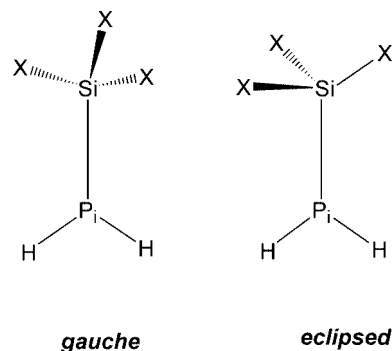


Figure 5. *Gauche* and *eclipsed* transition structures for monophosphanes H_2PCX_3 and H_2PSiX_3 .

Diphosphanes can be considered as phosphanyl substituted monophosphanes. Because of the small electronegativity difference between H and P, H_2PPHR and H_2PR molecules should have similar inversion barriers, and 1,2-disilylated diphosphanes should have smaller inversion barriers, than those of H_2PPH_2 and the alkylated derivatives RHPHR. To some extent, the results summarized in Table 2 confirm these expectations. Silyl substituents do lower ΔE_{inv} , and the PH_2 substituent lowers it less than the silyl group SiH_3 . Both effects (PH_2 : -32 kJ mol^{-1} ; SiH_3 : -44 kJ mol^{-1}) are roughly additive, as can be seen for $\text{SiH}_3\text{-PH-PH-SiH}_3$. The calculated barrier is $\approx 80 \text{ kJ mol}^{-1}$, the predicted value is $\approx 73 \text{ kJ mol}^{-1}$.

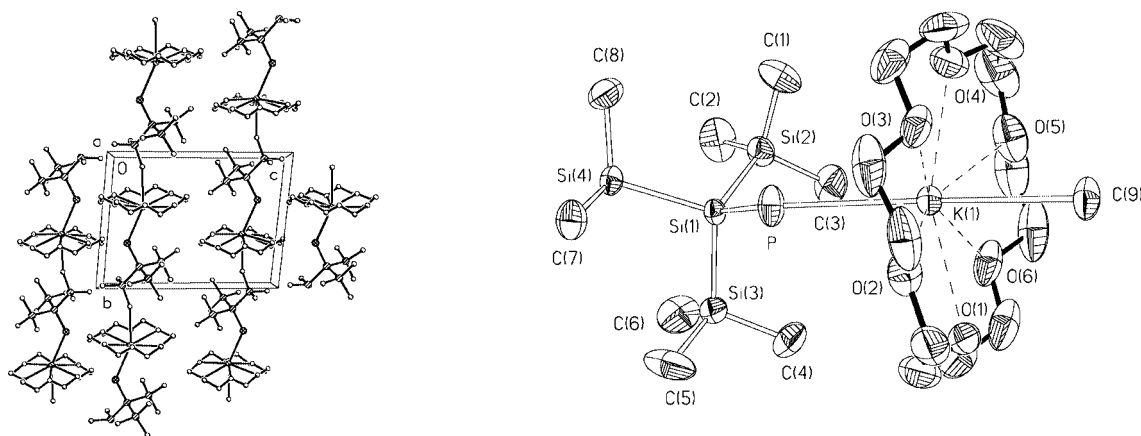
X-ray Crystallography

Compounds **3**, **4**, **12**, **13** and **14** were subjected to single-crystal X-ray analysis; details of the data collection and crystal data have been summarized in the Experimental Section. Selected bond lengths, bond angles and torsion angles are presented in Table 3.

The molecular structure of the 18-crown-6 salt of potassium phosphanide **4** and the arrangement of the molecules in the crystal is presented in Figure 6. Structural reports for potassium phosphanides are available for a small number of compounds only. Examples are $\text{K}(\text{thf})\text{P}(\text{SiMe}_3)_2$, which displays a ladder-type structure,^[22] $\text{KHPSi}(\text{Bu}_3)_3$,^[34] polymeric KHPMe_3^* ($\text{Me}_3^* = 2,4,6\text{-tBu}_3\text{C}_6\text{H}_2$)^[35] and dimeric $[\text{K}(\text{thf})_2\text{P}(2,4,6\text{-Me}_3\text{C}_6\text{H}_2)\text{SiF}(\text{tBu})_2]_2$.^[36] Because of the large size of the hypersilyl group and the presence of 18-crown-6, each phosphorus atom in **4** is coordinated to one potassium atom only, which is different from the above-mentioned examples where coordination numbers two or three are observed. The potassium phosphorus distance (see Table 3) is 326 pm, which compares well with values between 320–360 pm which are reported in the literature. Each potassium atom, in addition to being coordinated to the P atom and the crown ether, has a contact [$d_{\text{P-C}} = 335 \text{ pm}$] with a methyl group from the hypersilyl group of a

Table 3. Selected bond lengths [pm], bond angles [°] and dihedral angles [°] with estimated standard deviations in parentheses for **3**, **4**, **12**, **13** and **14**.

	3	4	12	13	14
P–P	–	–	220.2(3)	219.61(18)	215.90(40)
P–K	–	326.19(13)	–	–	–
P–Si _(Hyp)	231.56(8)	221.36(13)	226.86(18)	229.31(20)	230.10(40)
P–Si _(Me)	228.7(11)	–	–	225.80(20)	–
Si–Si	240.19(9)	233.19(13)	234.31(17)	237.35(20)	237.80(40)
	241.60(10)	233.36(15)	234.63(17)	237.85(20)	233.00(40)
	242.61(11)	234.35(12)	235.16(16)	238.95(20)	239.00(40)
P–C	–	–	–	–	188.9(10)
P–P–Si _(Hyp)	–	–	102.49(9)	109.11(8)	109.47(15)
P–P–Si _(Me)	–	–	–	115.98(8)	–
P–Si–Si	108.04(3)	107.30(5)	108.19(7)	109.29(8)	104.65(16)
	121.64(3)	110.17(6)	101.42(7)	123.29(8)	130.40(16)
	103.52(4)	112.39(5)	112.26(7)	106.47(9)	104.65(16)
Si _(Me) –P–Si _(Hyp)	108.55(3)	–	–	109.14(8)	–
	113.77(4)	–	–	–	–
C–P–Si _(Hyp)	–	–	–	–	110.20(40)
P–P–C	–	–	–	–	115.55(40)
Si _(Hyp) –P–P–Si _(Hyp)	–	–	180.0	139.27(7)	162.48(14)
Si _(Me) –P–P–Si _(Me)	–	–	–	26.66(11)	–
C–P–P–C	–	–	–	–	52.50(50)

Figure 6. Molecular structure of the 18-crown-6 salt of **4** and arrangement in the crystal.

neighbouring molecule. The structure thus displays a zig-zag chain $[\text{PKC}(\text{H}_3)\text{SiSi}]_n$, as shown in Figure 6. Noteworthy, the P–Si–Si angles within the hypersilyl group differ by not more than 5° from each other, which is due to the absence of steric strain. Moreover, the three Si–Si distances in the hypersilyl group are almost equal (233–234 pm), and they are the shortest compared those found for **3**, **12**, **13** and **14**.

The molecular structures of compounds **3**, **12**, **13** and **14** are presented together in Figure 7. The presence of two trimethylsilyl groups in **3** certainly increases the steric strain, which leads to quite long Si–P (231.6 and 228.7 pm) and Si–Si bonds (240.2–242.6 pm). The hypersilyl group is quite severely distorted from local C_3 symmetry, with P–Si–Si angles of 108.0°, 121.6° and 103.5°, respectively.

The strain in bis(hypersilyl)diphosphane **12** is considerably smaller than that in **3**, which results in shorter Si–P and Si–Si bonds and smaller variations in the P–Si–Si bond angles (Table 3). The two hydrogen atoms which are attached to the phosphorus atoms are located well inside the molecule and have no noticeable effect on the Si–P–P–Si dihedral angles that the diastereomers possess in the crystal form. Both the *meso*- and the *D,L*-diastereomers are present, which we corroborated by dissolving a single crystal in toluene and recording a ^{31}P NMR spectrum.

Despite the bulkiness of the substituents that diphosphanes **13** and **14** bear, the P–P bond lengths (220 and 216 pm, respectively) are in a range considered as normal. However, P–Si and Si–Si bonds are longer than those found for **4** and **12**. The X-ray structures together with the ^{31}P NMR spec-

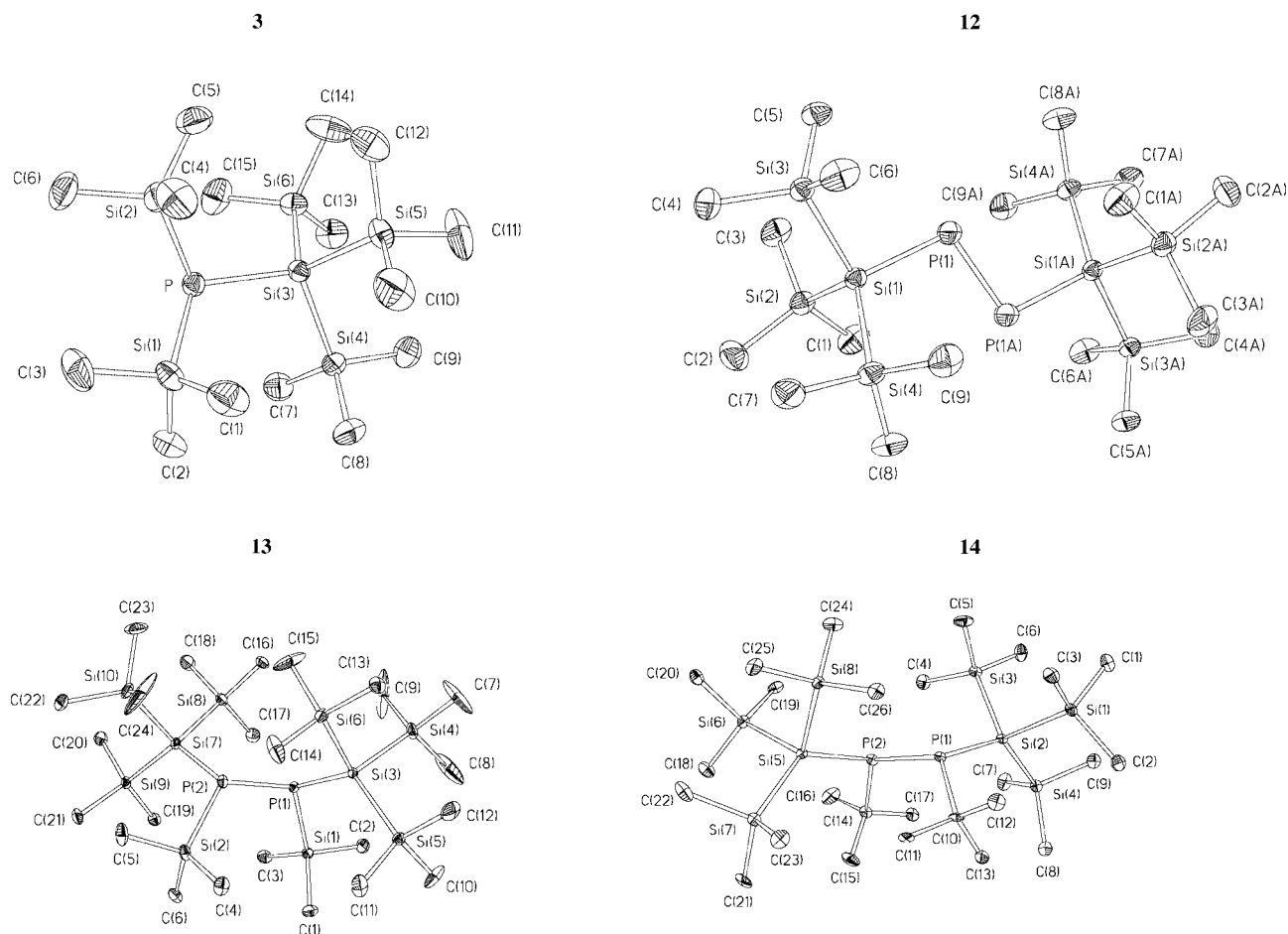


Figure 7. ORTEP plots (30% probabilities) of the molecular structures of **3**, **12**, **13** and **14**.

tra prove that it is the D,L-modifications which are formed exclusively. We were unable to detect even traces of the *meso*-diastereomers. Similar observations were made during the synthesis of $(\text{SiMe}_3)\text{PhPPP}(\text{SiMe}_3)$, $(\text{SiMe}_3)t\text{BuPP}t\text{Bu}(\text{SiMe}_3)$ and $t\text{BuPhPPP}t\text{Bu}$. All three diphosphanes display a single resonance in the ^{31}P NMR spectrum, but it is not clear in all three cases whether it originates from the *meso*- or the D,L-diastereomers.^[37]

Experimental Section

NMR Spectroscopy: NMR spectra were recorded with a BRUKER MSL 300 or a VARIAN Unity Inova 300 spectrometer. The ^{29}Si NMR and ^{31}P NMR spectra of the samples were measured as solutions in THF or toluene in 10 mm tubes with capillaries of D_2O to serve as an external lock.

X-ray Structure Analysis: The crystals were mounted onto the tip of a glass fibre, and the data collection was performed with a BRUKER-AXS SMART APEX CCD diffractometer. Graphite-monochromated $\text{Mo-K}\alpha$ radiation (71.073 pm) was used for the measurements. The data were reduced to F^2 , and corrected for absorption effects with SAINT and SADABS, respectively. The structures were solved by direct methods and refined by full-matrix least-squares method (SHELXL97). All non-hydrogen atoms were refined with anisotropic displacement parameters. All hydrogen atoms were located in calculated positions to correspond to stan-

dard bond lengths and angles. Relevant data are presented in Table 4. Because of the formation of thin plates, the quality of the structure data for **13** and **14** is poor. All attempts to obtain better crystals failed.

CCDC-605545 (for **3**), -605546 (for **4**), -605542 (for **12**), -605543 (for **13**) and -605544 (for **14**) contain the supplementary crystallographic data for this paper. These data can be obtained free of charge from The Cambridge Crystallographic Data Centre via www.ccdc.cam.ac.uk/data_request/cif.

Ab Initio Calculations: For geometry optimization, the B3LYP/6-31G(d) method has been applied as implemented in the GAUSSIAN package programs.^[38] In the population analysis, the Mulliken method was conducted for both phosphorus atoms.^[39] Unless otherwise stated, the optimized structures are minima on the potential energy hypersurfaces (only positive harmonic frequencies at the B3LYP/6-31G(d)//B3LYP/6-31G(d) level). The considered transition structures, TS, were characterized by a single vibration mode of inversion character at phosphorus.

General Remarks for the Syntheses: All syntheses and manipulations were carried out under an inert atmosphere of either N_2 or Ar with the use of standard Schlenk techniques. Solvents were distilled from sodium, potassium, sodium-potassium alloy or LiAlH_4 prior to use. Amines such as NEt_3 were dried with molecular sieves. Elemental analyses were performed with a HERAEUS Vario Elemental.

Synthesis of HypPH₂ (1) and Hyp₂PH (2) from NaPH₂ and $(\text{SiMe}_3)_3\text{SiCl}$: HypCl (13.6 g, 48.1 mmol) was dissolved in a mix-

Table 4. Crystal data and structure refinement for compounds **3**, **4**, **12**, **13** and **14**.

	3	4	12	13	14
Formula	C ₁₅ H ₄₅ PSi ₆	C ₂₁ H ₅₂ KO ₆ PSi ₄	C ₁₈ H ₅₆ P ₂ Si ₈	C ₂₄ H ₇₂ P ₂ Si ₁₀	C ₂₆ H ₇₂ P ₂ Si ₈
Formula weight	425.02	583.06	559.19	703.66	671.495
<i>T</i> [K]	213(1)	293(2)	200(2)	100(2)	100(2)
Wavelength [Å]	0.71073	0.71069	0.71073	0.71073	0.71073
Crystal system	monoclinic	triclinic	triclinic	triclinic	triclinic
Space group	<i>C2/c</i>	<i>P</i> $\bar{1}$	<i>P</i> $\bar{1}$	<i>P</i> $\bar{1}$	<i>P</i> $\bar{1}$
<i>a</i> [Å]	15.707(3)	9.7417(19)	9.5970(19)	10.191(2)	9.6834(19)
<i>b</i> [Å]	11.599(2)	11.839(2)	13.266(3)	13.097(3)	14.090(3)
<i>c</i> [Å]	33.006(7)	15.711(3)	15.805(3)	17.971(4)	16.090(3)
α [°]	90.0	94.59(3)	81.28(3)	98.62(3)	79.58(3)
β [°]	100.91(3)	94.19(3)	84.79(3)	97.98(3)	89.44(3)
γ [°]	90.0	101.88(3)	69.44(3)	103.98(3)	74.00(3)
<i>V</i> [Å ³]	5904(2)	1759.9(6)	1860.7(6)	2262.7(8)	2073.6(7)
<i>Z</i>	8	2	2	2	2
$\rho_{\text{calcd.}}$ [g cm ⁻³]	0.956	1.100	0.998	1.033	1.075
Absorption coefficient [mm ⁻¹]	0.335	0.360	0.381	0.375	0.351
<i>F</i> (000)	1872	632	612	772	740
θ range [°]	1.26 < θ < 23.25	1.77 < θ < 23.26	1.97 < θ < 24.71	1.17 < θ < 25.00	1.29 < θ < 22.00
<i>h</i> , <i>k</i> , <i>l</i> Indices range	−17 < <i>h</i> < 17 −12 < <i>k</i> < 12 −36 < <i>l</i> < 38	−10 < <i>h</i> < 10 −13 < <i>k</i> < 12 −17 < <i>l</i> < 17	−11 < <i>h</i> < 11 −15 < <i>k</i> < 15 −18 < <i>l</i> < 18	−12 < <i>h</i> < 12 −15 < <i>k</i> < 15 −21 < <i>l</i> < 21	−10 < <i>h</i> < 10 −14 < <i>k</i> < 14 −16 < <i>l</i> < 16
Reflections collected / unique	17157 / 4228	10812 / 5020	13046 / 6278	15965 / 7821	11017 / 5005
Completeness to θ [°]/[%]	23.25/99.7	23.26/99.3	24.71/98.7	25.00/98.2	22.00/98.4
Absorption correction	SADABS	SADABS	SADABS	SADABS	SADABS
Refinement method	Full-matrix least-squares on <i>F</i> ²	Full-matrix least-squares on <i>F</i> ²	Full-matrix least-squares on <i>F</i> ²	Full-matrix least-squares on <i>F</i> ²	Full-matrix least-squares on <i>F</i> ²
Data/restraints/parameters	4228/0/214	5020/0/322	6278/0/279	7821/0/349	5005/0/349
Goodness-of-fit on <i>F</i> ²	1.064	1.032	1.017	1.1312	1.143
Final <i>R</i> indices [<i>I</i> > 2 σ (<i>I</i>)]	<i>R</i> 1 = 0.0370 <i>wR</i> 2 = 0.0995	<i>R</i> 1 = 0.0492 <i>wR</i> 2 = 0.1285	<i>R</i> 1 = 0.0622 <i>wR</i> 2 = 0.1208	<i>R</i> 1 = 0.0881 <i>wR</i> 2 = 0.2038	<i>R</i> 1 = 0.1235 <i>wR</i> 2 = 0.3025
<i>R</i> indices (all data)	<i>R</i> 1 = 0.0422 <i>wR</i> 2 = 0.1024	<i>R</i> 1 = 0.0575 <i>wR</i> 2 = 0.1352	<i>R</i> 1 = 0.0936 <i>wR</i> 2 = 0.1343	<i>R</i> 1 = 0.0939 <i>wR</i> 2 = 0.2078	<i>R</i> 1 = 0.1406 <i>wR</i> 2 = 0.3145
Largest diff. peak/hole [e Å ⁻³]	0.238/−0.152	0.328/−0.160	0.440/−0.275	1.315/−1.041	1.301/−0.678

ture of toluene (30 mL) and Et₂O (30 mL). NaPH₂ (5.4 g, 96.2 mmol) was then added, and the suspension was heated at reflux for 2 d. ²⁹Si NMR spectroscopy was used to monitor the consumption of HypCl. Upon completion, the liquid phase which contained **1** and **2** and traces of Hyp₃P₇ was separated from the salts (NaCl) by decantation. The solvent was then removed by evaporation in vacuo. From the oily residue, **1** was separated by fractional distillation, b.p. 65–68 °C (0.03 mbar). It solidified at room temperature to a colourless sticky wax. From the residue, **2** (1.4 g, 11%) can be obtained by sublimation in vacuo at a temperature of 120–125 °C. Compound **2** can also be prepared from HypPHK and HypCl in excellent yield (see later on). Yield of **1** 7.4 g (55%). C₉H₂₉PSi₄ (280.66): calcd. C 38.51, H 10.41; found C 38.70, H 9.70.

Synthesis of HypPH₂ (1) from PH₃, HOSO₂CF₃, and (SiMe₃)₃-SiPh: (SiMe₃)₃SiPh (10 g, 28.1 mmol) was dissolved in toluene (50 mL). The solution was cooled to −30 °C, and CF₃SO₃H (4.21 g, 28.1 mmol) was added dropwise over a period of one hour. The reaction mixture was warmed up to room temperature and was stirred for another 2 h. Triethylamine (2.84 g, 28.1 mmol) was then added, and a moderate stream of PH₃ was passed through the solution. Immediately, a colourless oil of [CF₃SO₃][−][NHEt₃]⁺ formed. After completion, the solution of HypPH₂ was separated from the oil by decantation. The solvent then was removed by evaporation in vacuo, and **1** was purified by sublimation as described previously. Yield 75%.

Synthesis of HypPHK (4): Compound **1** (0.5 g, 1.80 mmol) was dissolved in toluene (10 mL) and cooled to −50 °C. With vigorous

stirring, KO^tBu (0.22 g, 2.0 mmol) and 18-crown-6 (0.52 g, 2.0 mmol) was added with a spatula. The solution turned yellow/orange slowly. After 2 h, the reaction was complete. Product **4** crystallized from toluene at −80 °C in the form of yellow crystals that were suitable for X-ray analysis. Yield 0.38 g (≈ 60%).

Synthesis of Hyp₂PH (2) from 4 and HypCl: Compound **4** (2.0 mmol; prepared from 0.6 g of **1** as described above) was dissolved in toluene (10 mL). The solution was vigorously stirred and a solution of HypCl (0.56 g, 2.0 mmol) in toluene (10 mL) was added slowly at a temperature of −40 °C. After one hour, the mixture was warmed up to room temperature. The liquid phase was separated from the salts by decantation. Sublimation in vacuo (0.03 mbar, 120–125 °C) afforded **2** (2.46 g, 80%) as a colourless waxy solid. M.p. 160 °C. C₁₈H₅₅PSi₈ (527.33): calcd. C 41.00, H 10.51; found C 39.79, H 9.94.

Synthesis of HypPHLi (6): HypPH₂ (1.67 g, 5.95 mmol) was dissolved in THF (20 mL) and cooled with ice to 0 °C. With constant stirring, *n*BuLi (5.95 mmol, hexane solution) was added with a syringe. The solution turned red slowly. Compound **6** (≈ 95%) was afforded, and traces of (Me₃Si)₂PLi, Li₃P₇ and HypPLi₂ (**7**) could be detected in the solution by ³¹P NMR spectroscopy.

Synthesis of HypP(SiMe₃)K (5): HypP(SiMe₃)₂ (1.28 g, 3.01 mmol) was dissolved in toluene (60 mL). The solution was cooled to −50 °C and KO^tBu (0.34 g, 3.03 mmol) and 18-crown-6 (0.80 g, 3.03 mmol) was added as a solid. The solution turned orange slowly. After two hours the reaction was complete. From analysis of the ³¹P NMR spectrum, a yield of ≈ 95% could be deduced. Minor byproducts were HypPK₂ and HypPHK.

Synthesis of HypP(SiMe₃)H: HypP(SiMe₃)₂ (0.33 g, 0.78 mmol) was dissolved in toluene (60 mL). Dry *t*BuOH (0.06 g) was then added, and the reaction mixture was stirred for three weeks at room temperature. Analysis of the ³¹P NMR spectrum revealed a 1:1 mixture of HypP(SiMe₃)H and the starting material. If the reaction was heated at 100 °C under a vacuum of 0.03 mbar, HypP(SiMe₃)H was obtained as a waxy, colourless solid. C₁₂H₃₇PSi₅ (352.86): calcd. C 40.85, H 10.57; found C 39.70, H 10.33.

Synthesis of HypPHHPHyp (12): HypPH₂ (1) (12.1 g, 43.1 mmol) was dissolved in toluene (100 mL). With vigorous stirring, (*t*Bu)₂Hg (8.0 g, 26.0 mmol) was added at room temperature. The solution was then heated at 60 °C. After 2 h, a small quantity of mercury had formed and the colour of the solution had turned to a yellowish-green. At -80 °C, crystals of HypPHHPHyp precipitated as yellow needles. Yield 10.8 g (90%).

Alternatively, **1** (1.0 g, 4.0 mmol) was dissolved in toluene (15 mL) and solid KO*t*Bu (0.5 g, 4.5 mmol) and solid 18-crown-6 (1.2 g, 4.5 mmol) was added at -50 °C. The solution turned yellow slowly. After 3 h at -50 °C, BrCH₂CH₂Br (0.43 g, 2.25 mmol) was added. The colour changed immediately to a yellowish-green. The solution was decanted from the salts and stored in a freezer at -80 °C where **12** (1.00 g, 90%) crystallized. C₁₈H₅₆P₂Si₈ (559.33): calcd. C 38.65, H 10.09; found C 37.60, H 9.41.

Synthesis of Hyp(SiMe₃)PP(SiMe₃)Hyp (13): HypP(SiMe₃)₂ (**3**) (1.00 g, 2.35 mmol) was dissolved in toluene (30 mL). With vigorous stirring, solid KO*t*Bu (0.30 g, 2.67 mmol) and solid 18-crown-6 (0.70 g, 2.65 mmol) was added at -50 °C. The solution turned yellow immediately. After three hours the reaction mixture was warmed up to room temperature. The solution of Hyp(SiMe₃)PK then was again cooled to -50 °C and BrCH₂CH₂Br (0.25 g, 1.33 mmol) was added. The colour of the solution slowly turned green. After one hour, the salts were separated by decantation and the solution was stored in a freezer at -80 °C. Product **13** (0.62 g, 65%) crystallized as yellowish thin plates. C₂₄H₇₂P₂Si₁₀ (703.70): calcd. C 40.96, H 10.31; found C 41.40, H 10.26.

Synthesis of Hyp(*t*Bu)PP(*t*Bu)Hyp (14): *t*BuPClHyp (1.00 g, 2.70 mmol) was dissolved in toluene (20 mL). With vigorous stirring, K/Na alloy (5:1; 0.20 g, excess) was added with a syringe at room temperature. The solution was then heated at 80 °C for three hours. The liquid phase was separated from the salts by decantation and stored at -80 °C in a freezer. Product **14** (0.73 g, 80%) was obtained as yellowish thin plates. C₂₆H₇₂P₂Si₈ (671.55): calcd. C 46.50, H 10.72; found C 45.48, H 10.11.

Synthesis of HypPCl(SiMe₃) (8): HypP(SiMe₃)₂ (**3**) (1.54 g, 3.62 mmol) was dissolved in toluene (20 mL). With vigorous stirring solid C₂Cl₆ (0.86 g, 3.63 mmol) was added, at room temperature. The reaction proceeds slowly and is complete after 24 h at room temperature. After removal of all volatile products by evaporation in vacuo, a nearly pure **8** (1.27 g, 92%) is obtained as a viscous yellowish oil. Further purification by sublimation turned out to be impossible as the compound decomposed quickly when warmed. Attempts to obtain crystals were unsuccessful. C₁₂H₃₆ClPSi₅ (387.30): calcd. C 37.21, H 9.37; found C 36.59, H 8.86.

Synthesis of HypPCl₂ (10): HypP(SiMe₃)₂ (**3**) (0.27 g, 0.64 mmol) was dissolved in toluene (20 mL) and solid C₂Cl₆ (0.35 g, 1.45 mmol) was added with a spatula. After 24 h at room temperature and under vigorous stirring, the reaction was complete. Analysis of the ³¹P NMR spectrum revealed that besides HypPCl₂ (≈ 70%), cyclotriphosphane P₃Hyp₂Cl (≈ 15%) and bis(hypersilyl)-bicyclotetraphosphane P₄Hyp₂ (≈ 15%) were also present in the

reaction mixture. Attempts to isolate or purify **10** by fractional crystallization were not successful.

Synthesis of HypP(SiMe₃)Br (9): HypP(SiMe₃)₂ (**3**) (1.00 g, 2.35 mmol) was dissolved in toluene (30 mL) and solid BrCl₂CCCl₂Br (0.76 g, 2.35 mmol) was added with a spatula. After two hours at room temperature and vigorous stirring, the reaction was complete. All volatile products were then removed by evaporation in vacuo. Pure **9** (1.0 g, ≈ 100%) was obtained as a yellowish waxy solid. Further purification by sublimation was impossible due to decomposition. Attempts to obtain crystals were also unsuccessful. C₁₂H₃₆BrPSi₅ (431.75): calcd. C 33.38, H 8.40; found C 32.49, H 8.33.

Synthesis of HypPBr₂ (11): HypP(SiMe₃)₂ (**3**) (0.23 g, 0.54 mmol) was dissolved in toluene (10 mL) and solid BrCl₂CCCl₂Br (0.35 g, 1.08 mmol) was added with a spatula. The colour of the solution turned a yellowish brown. After two hours at room temperature, the reaction was complete. All volatile products were removed by evaporation in vacuo to afford **11** (0.22 g, 95%) of a yellow, viscous oil. Noticeable amounts of byproducts could not be detected in the analysis of the ³¹P NMR spectrum. C₉H₂₇Br₂PSi₄ (438.47): calcd. C 24.65, H 6.21; found C 22.87, H 5.26.

Acknowledgments

Financial support by the "Fonds zur Förderung der wissenschaftlichen Forschung", Vienna, is gratefully acknowledged (project P 18176-N11).

- [1] Hypersilane and supersilane were proposed as trivial names for tris(trimethylsilyl)silane and tri(*tert*-butyl)silane by N. Wiberg during the Xth International Symposium on Organosilicon Chemistry in Poznan, Poland 1993.
- [2] T. Gross, H. Reinke, H. Oehme, *Can. J. Chem.* **2000**, *78*, 1399–1404.
- [3] H. Bock, J. Meuret, R. Baur, K. Ruppert, *J. Organomet. Chem.* **1993**, *446*, 113–122.
- [4] F. H. Elsner, T. D. Tilley, *J. Am. Chem. Soc.* **1988**, *110*, 313–314.
- [5] K. W. Klinkhammer, *Chem. Eur. J.* **1997**, *3*, 1418–1431.
- [6] M. Westerhausen, W. Schwarz, *Z. Anorg. Allg. Chem.* **1993**, *619*, 1053–1063.
- [7] M. Westerhausen, M. Wienieke, B. B. Rademacher, W. Schwarz, *Chem. Ber./Recueil* **1997**, *130*, 1499–1505.
- [8] M. Westerhausen, J. Greul, H.-D. Hausen, W. Schwarz, *Z. Anorg. Allg. Chem.* **1996**, *622*, 1295–1305.
- [9] A. H. Cowley, T. H. Newman, *Organometallics* **1982**, *1*, 1412–1413.
- [10] T. W. Kim, W. S. Jahng, C. H. Kim, M. E. Lee, *Rapid Commun. Mass Spectrom.* **1993**, *7*, 898–901.
- [11] S. Haber, M. Schmitz, U. Bergsträßer, J. Hoffmann, M. Regitz, *Chem. Eur. J.* **1999**, *5*, 1581–1589.
- [12] M. Haase, U. Klingebiel, *Z. Naturforsch. Teil B* **1986**, *41*, 697–701; M. Haase, U. Klingebiel, L. Skoda, *Z. Naturforsch. Teil B* **1984**, *39*, 1500–1504.
- [13] J. Hein, C. Gärtner-Winkhaus, M. Nieger, E. Niecke, *Heteroat. Chem.* **1991**, *2*, 409–415.
- [14] J. Markov, R. Fischer, H. Wagner, N. Noormofidi, J. Baumgartner, C. Marschner, *Dalton Trans.* **2004**, *14*, 2166–2169.
- [15] K. Hassler, *J. Organomet. Chem.* **1988**, *348*, 33–39.
- [16] H. Siegl, W. Krumlacher, K. Hassler, *Monatsh. Chem.* **1999**, *130*, 139–145.
- [17] J. Baumgartner, V. Cappello, A. Dransfeld, K. Hassler in *Silicon Chemistry, From the Atom to Extended Systems* (Eds.: P. Jutzi, U. Schubert), Wiley-VCH, Weinheim **2004**.

- [18] W. Uhlig, *Z. Anorg. Allg. Chem.* **1990**, 588, 133–138.
- [19] U. Baumeister, K. Schenzel, R. Zink, K. Hassler, *J. Organomet. Chem.* **1997**, 543, 117–124.
- [20] G. Brauer, *Handbuch der präparativen Anorganischen Chemie*, Ferdinand Enke, Stuttgart, **1975**.
- [21] G. Fritz, J. Härer, K. H. Schneider, *Z. Anorg. Allg. Chem.* **1982**, 487, 44–58.
- [22] U. Englisch, K. Hassler, K. Ruhland-Senge, F. Uhlig, *Inorg. Chem.* **1998**, 37, 3532–3537.
- [23] R. Appel, W. Paulen, *Angew. Chem. Int. Ed. Engl.* **1981**, 20, 869–870.
- [24] V. Cappello, J. Baumgartner, A. Dransfeld, M. Flock, K. Hassler, *Eur. J. Inorg. Chem.* **2006**, 2393–2405.
- [25] M. Baudler, G. Hoffmann, M. Hallab, *Z. Anorg. Allg. Chem.* **1980**, 466, 71–75.
- [26] for instance, see A. H. Cowley, W. D. White, *J. Am. Chem. Soc.* **1969**, 91, 1913–1917; J. P. Albrand, D. Gagnaire, J. B. Robert, *J. Am. Chem. Soc.* **1973**, 95, 6498–6500; J. P. Albrand, J. B. Robert, *J. Chem. Soc. Chem. Commun.* **1974**, 16, 644–645; J. P. Albrand, H. Faucher, D. Gagnaire, J. B. Robert, *Chem. Phys. Lett.* **1976**, 38, 521–523.
- [27] Private communication with M. Flock, unpublished results.
- [28] M. Baudler, C. Gruner, H. Tschäbunin, J. Hahn, *Chem. Ber.* **1982**, 115, 1739–1745.
- [29] H. Günther, *NMR Spektroskopie*, Georg Thieme, Stuttgart/N. Y., **1983**.
- [30] R. D. Baechler, K. Mislow, *J. Am. Chem. Soc.* **1970**, 92, 4758–4759.
- [31] R. D. Baechler, K. Mislow, R. J. Cook, G. H. Senkler, *J. Am. Chem. Soc.* **1972**, 94, 2859–2861.
- [32] A. Rauk, J. D. Andose, W. G. Frick, R. Tang, K. Mislow, *J. Am. Chem. Soc.* **1971**, 93, 6507–6515; C. C. Levin, *J. Am. Chem. Soc.* **1975**, 97, 5649–5655.
- [33] A. Dransfeld, Thesis, Erlangen, **1998**.
- [34] M. Westerhausen, S. Weinrich, B. Schmid, S. Schneiderbauer, M. Suter, H. Nöth, H. Piotrowski, *Z. Anorg. Allg. Chem.* **2003**, 629, 625–633.
- [35] G. W. Raabe, G. P. A. Yap, A. L. Rheingold, *Inorg. Chem.* **1997**, 36, 1990–1991.
- [36] M. Andrianarison, D. Stalke, U. Klingebiel, *Chem. Ber.* **1990**, 123, 71–73.
- [37] H. Schumann, R. Fischer, *J. Organomet. Chem.* **1975**, 88, C13–C16; M. Baudler, M. Hallab, A. Zarkadas, E. Tolls, *Chem. Ber.* **1973**, 106, 3962–3969.
- [38] M. J. Frisch, G. W. Trucks, H. B. Schlegel, G. E. Scuseria, M. A. Robb, J. R. Cheeseman, J. A. Montgomery Jr., T. Vreven, K. N. Kudin, J. C. Burant, J. M. Millam, S. S. Iyengar, J. Tomasi, V. Barone, B. Mennucci, M. Cossi, G. Scalmani, N. Rega, G. A. Petersson, H. Nakatsuji, M. Hada, M. Ehara, K. Toyota, R. Fukuda, J. Hasegawa, M. Ishida, T. Nakajima, Y. Honda, O. Kitao, H. Nakai, M. Klene, X. Li, J. E. Knox, H. P. Hratchian, J. B. Cross, C. Adamo, J. Jaramillo, R. Gomperts, R. E. Stratmann, O. Yazyev, A. J. Austin, R. Cammi, C. Pomelli, J. W. Ochterski, P. Y. Ayala, K. Morokuma, G. A. Voth, P. Salvador, J. J. Dannenberg, V. G. Zakrzewski, S. Dapprich, A. D. Daniels, M. C. Strain, O. Farkas, D. K. Malick, A. D. Rabuck, K. Raghavachari, J. B. Foresman, J. V. Ortiz, Q. Cui, A. G. Baboul, S. Clifford, J. Cioslowski, B. B. Stefanov, G. Liu, A. Liashenko, P. Piskorz, I. Komaromi, R. L. Martin, D. J. Fox, T. Keith, M. A. Al-Laham, C. Y. Peng, A. Nanayakkara, M. Challacombe, P. M. W. Gill, B. Johnson, W. Chen, M. W. Wong, C. Gonzalez, J. A. Pople, *GAUSSIAN03/Revision C.02*, Gaussian, Inc., Wallingford CT, **2004**.
- [39] R. S. Mulliken, *J. Phys. Chem.* **1962**, 36, 3428–3439.

Received: May 12, 2006

Published Online: October 2, 2006